9 GROUND-ACOUSTIC TESTING

Flights 91 to 99 were flown at the Crows Landing Naval Auxiliary Airfield near Patterson, California. The primary purpose of these tests was to obtain acoustic measurements of the radiated noise from the UH–60A aircraft, simultaneously with onboard measurement of the blade pressures. Ames Research Center personnel were responsible for acquiring and reducing the flight data and Langley Research Center personnel were responsible for acquiring and reducing the acoustic data. The basic flight procedures for this portion of the program are discussed in Section 2. Details of the acoustic instrumentation, data reduction, and results are reported in Refs. 6 to 8.

The normal data reduction process was modified for the ground-acoustic testing portion of the Airloads Program. A two-step procedure was established in which aircraft data for the entire record, excluding the rotor measurements, were combined with laser and radar tracking information and placed in the BH2 (Ames) data base. These data were stored with a prefix 4 to avoid confusion with counters that were subsequently processed and installed in the same data base. Thus, the full record for Counter 9104, but without rotor measurements, is accessible as Counter 49104. In the second step, one or more segments of the prefix-4 records were selected by Ames personnel for installation in the BH2 data base and these records do include the rotor measurements. The selection criteria used were the same as for other data records in the flight program, that is, five seconds of data were selected from the steadiest portion of the data record. In this second step, a number of data segments were also selected by Langley personnel and these were installed in the BHL data base, again to include the rotor measurements. Different criteria were used by Langley in selecting appropriate time slices for the BHL data base. In particular, for the Langley data base it was important that the data be acquired when the aircraft was near or over the acoustic array. Note that the BHL data base includes only the aircraft data for these test conditions. The acoustic data are stored separately at Langley Research Center.

The ground-acoustic testing was divided into two parts. In the first part a “standard” microphone array was used to record the acoustic data. This standard array is illustrated in Fig. 79a and the x- and y-position data are given in Table 110. The spacing of this array was designed to provide 10 deg angular resolution for the aircraft flying at 250 feet over the center of the array (Ref. 6). For this first portion of the testing, data were obtained for steady level flight over the array, climbs and descents, and hover. These tests are discussed below in the sections “Level Flight,” “Climbs and Descents,” and “Hover.”

The second part of the ground-acoustic testing examined aircraft noise in maneuvering flight. For this portion of the testing, a “non-standard” microphone array was used as shown in Fig. 79b and the position data are also in Table 110. The microphone layout for these tests used linear spacing. Two types of maneuvers were investigated in this second portion of the testing. The first type was a heading turn in which the aircraft approached the microphone array center on one heading and then turned over the microphones and exited at a new heading. These heading changes ranged from 15 to 90 deg and two levels of aggressiveness were used. These turns are discussed below in the section “Moderate and Aggressive Heading Turns.” The second maneuver was a constant radius turn centered on the microphone array. Three different radii were used for these turns and are discussed in the section “Constant Radius Turns.”

Level Flight

Twenty-three level flight data records were obtained during the ground-acoustic testing and the prefix-4 counters are listed in Table 39 (Section 6). Of the twenty-three cases, segments of seven were reduced for the BHL data base. The time slices used for the seven counters are shown in Table 111 and the counters are listed in Table 112. The level flight counters range in airspeed from 41 to 145 KIASB.

Position measurements using the laser tracker were successfully obtained for six of the seven level flight counters in Table 112, and the z- and y-position data as a function of the x-position are shown in Fig. 80. These data were extracted from the TRENDS data base using the OUTDATA utility as a batch process under GATEWAY in the TRENDS menu. The tracking data were then post-processed to compute the average x-, y-, and z-position of the aircraft for each rotor revolution and these mean position data are shown in the figure. Note that the data records are roughly symmetric with respect to the center of microphone array and are longer than the BH2 data base counters shown previously in Fig. 36. The flight path and tip-path-plane angles for the six level flight cases are shown in Table 113. The variance in the flight path angle is generally less than three to four degrees. However, for Counter 9204 the variance is 12.7 deg, largely because the aircraft started to descend a thousand feet past the microphone center and eventually dropped below 200 feet, as shown in Fig. 80.

Climbs and Descents

Thirty-one climb cases were obtained during the ground-acoustic testing as previously shown in Table 50. Of these cases, time slices for 17 counters were selected for the BHL data base. Table 114 shows the relationship of the BHL time slices to the prefix-4 data base. Details of the 17 BHL climb counters are listed in Table 115. Similarly, of the 39 descent cases obtained during ground-acoustic testing (see Table 53), 15 were selected for the BHL data base and the time slice relationships are shown in Table 116. Details of the 16 descent counters are listed in Table 117.

Laser and radar tracking data were successfully obtained for nearly all of the climb, level flight, and descent cases in the BHL data base. The x- and z-position data for these counters are shown in Fig. 81. These data were extracted from the TRENDS data base using the OUTDATA utility as a batch process under GATEWAY in the TRENDS menu. The tracking data were then post-processed to compute the average x- and z-position of the aircraft for each rotor revolution and these mean position data are shown in the figure. The center of the microphone array is located at $X = 0$ ft in the figure and this center point is indicated with a dashed vertical line. The ILS indicator in the cockpit was driven externally to provide guidance to the pilot so that the aircraft would pass over the microphone array centerline at an elevation of 250 ft. Greater variance in the flight path angle and the crossing elevation for the microphone array is observed for climbs than for level flight or descent. This greater variance reflects the difficulty the pilots encountered in transitioning to a climb from low altitude, with the need to maintain a steady climb rate and simultaneously pass through the 250-foot point over the center of the microphone array. This task was easier in descent as more time was available to set up on a steady descent rate. The lowest variance in elevation achieved over the microphone array was for the level flight cases.

The flight path angles for ascents, descents, and level flight were estimated by fitting a first-order regression curve to the x- and z-position data. The flight path angles are shown in Fig. 82 as a function of advance ratio for all of the BHL data base counters. The tip-path-plane angle was computed for these cases using the same method as discussed in Section 7. The tip-path-plane angles are shown in Fig. 83 as a function of advance ratio. The angles and estimates of variance are shown in Table 118 for the climbing flight cases and in Table 119 for the descent cases (and previously in Table 113 for level flight).

The variance is quite high for some of the flight path angles, particularly in climbing flight. The mean standard error of estimate for the climbing cases is 7.6 deg, while it is only 4.2 deg for the descending cases. Interestingly, the variance in the tip-path-plane angle is considerably less than the flight path angles. It is only 2.5 deg for climbing flight and 1.7 deg for descending flight. The tip-path-plane angle variance is probably more important than the flight path angle as concerns radiated acoustic noise. The variances for the same counters in the BH2 data base are considerably less and rarely exceed one degree (see Tables 42, 56, and 57).

This is a consequence of purposely selecting five-second segments from the steadiest portions of the flight records.

As shown in Fig. 83, the tip-path-plane angle of attack varies from about –15 deg in climbs to 10 deg in descents. At the high angles of attack in climb the induced flow is large and the blade tip vortices are convected away from the rotor. However, as the climb rate is reduced, the trailed tip vortices come closer to the rotor disk and eventually interact with subsequent blades, a phenomenon referred to as Blade Vortex Interaction (BVI). Eight cases at $\mu = 0.2$ have been selected from the climb, level flight, and descent data to show the effect of the tip-path-plane angle of attack on BVI. There is considerable variance in the tip-path-plane angle during these conditions, so a single revolution of data was selected for each counter where the data appeared relatively steady. These eight cases are listed in Table 120, which includes the tip-path-plane angle averaged over the entire record, the local tip-path-plane angle for the single revolution selected, and the time at which that revolution starts within the record. The pressure data were extracted from TRENDS using the OUTDATA utility and these data were converted to the Plot/Data Base format using post-processing routines. Figure 84 shows the normal force computed at 0.865*R* for the eight cases, where only harmonics above the 16th are retained, to clearly show the BVI on the rotor at this radial station. At the greatest climb rate, there is no indication of BVI in these measurements. As climb rate is reduced and the tip-path-plane increases, small BVIs are observed on the advancing side at the start of the second quadrant for $\alpha_{TPP} = -6.3$ deg. As the climb rate is further reduced, and the tip-path-plane angle of attack increases, multiple BVIs are seen on both the advancing and retreating sides. On the advancing side, multiple BVIs become stronger with increasing tip-path-plane angle and occur at earlier azimuth angles. On the retreating side, the BVIs occur later in azimuth and essentially disappear at the highest descent rate.

The extent of the BVIs at $\alpha_{TPP} = 5.2$ deg is examined in Fig. 85, which shows the filtered time histories over the nine radial blade stations for this relatively severe BVI case. On the advancing side the intensity of the BVIs and the number of interactions appears greatest from about 0.40*R* to 0.775*R*. On the retreating side, however, the BVIs appear strongest from 0.865*R* to 0.965*R*.

Hover

Sixteen hover records were obtained during the ground-acoustic testing and the prefix-4 counters are listed in Table 19 (Section 5). Of these records, time slices were selected for 13 flight cases to be installed in the BHL data base. The time slices used for the 13 counters are shown in Table 121 and the counters are listed in Table 122.

The pilot was assisted in maintaining position over the acoustic array by two observers on the ground using theodolites, as discussed previously in Section 5. As these ground observers were not protected from the laser used by the tracking system, only radar tracking daa were obtained. Previously, in Fig. 19, tracking data for the hover points in the BH2 data base were shown for the hover records. Tracking data for the hover points in the BHL data base are shown in Fig. 86 and appear nearly identical to the tracking data shown previously although different time slices are used in the two data bases. The variance for these hover cases, as estimated from one standard deviation of the radar tracking data, ranged from 0.4 to 4.3 feet for the x-position, 0.2 to 4.5 feet for the y-position, and 0.2 to 2.2 feet for the z-position.

The ground-acoustic hover test points were obtained in winds of six to 11 knots, as shown previously in Fig. 20. As the aircraft heading was changed by 15 deg between each test point, the relative wind at the aircraft also changed with each test point. In the discussion of these test points in Section 5 it was shown that there was substantial variation in the blade loading at various azimuths, depending upon the relative wind vector. Of the three sample cases shown in Fig. 23, the worst case appeared to be Counter 9406, where the relative wind was approaching from the right-rear quadrant. Figure 87 shows this same case, but where the normal force has been filtered to remove the 0–16 harmonics. The remaining harmonics are considered to be the most important as concerns acoustic noise. In this figure, substantial BVI noise is shown on the rotor, particularly in the fourth quadrant. Compared to the case of severe BVI loading in descending flight, shown in Fig. 84, the high-frequency BVI loading in hover is substantially greater (note the ordinate axis change).

Three vertical climb counters were obtained during the ground-acoustic testing, see Table 64, as shown previously. However, none of these cases were selected for time slices in the BHL data base.

Moderate and Aggressive Heading Turns

Acoustic measurements were obtained in heading turns over the microphone array where the aircraft approached the center of the array at one heading and then turned over that center point to exit the array at a different heading. Both moderate and aggressive turns were performed, the difference being the rapidity of the turn in the roll rate achieved upon entering and leaving the turn. This was discussed previously in Section 8, for example see Figs. 73 and 74. The heading change in these maneuvers ranged from 15 to 90 deg and turns to both left and right were flown.

Thirty-two moderate heading turns were flown during the ground-acoustic testing (see Table 96) and, of these, data were selected for the BHL data base for 13 counters. The time relationships of the data selected for the BHL data base to the prefix-4 data base are shown in Table 123. The moderate turn cases are listed in Table 124. Twenty-four aggressive heading turns were flown during the testing (see Table 98) and, of these, seven cases were selected for the BHL data base. The time relationships between the prefix-4 and BHL data bases are shown in Table 125. The aggressive heading turn counters in the BHL data base are listed in Table 126.

Two heading turns are selected for comparison in Fig. 88. Both heading turns are 60 deg to the right with an approach speed of 60 KIASB. The peak roll rate measured during the moderate heading turn, Counter 9908, was 13.6 deg/sec. The peak roll rate for the aggressive heading turn was 36.5 deg/sec. To indicate the potential for acoustic radiation, the normal force time history at 0.92R was filtered to show only harmonics of 17 and above, which are the primary contributors to BVI noise. The data in Fig. 88 are shown in a three-dimensional cycle plot where sequential azimuthal time histories are compared, and this provides an indication of the unsteadiness during the maneuver. There are 46 cycles or revolutions of data during the moderate maneuver, about 10.6 sec, and 41 cycles, about 9.4 sec, for the aggressive maneuver. It is interesting to note in Fig 88, that although the peak BVI normal force is slightly higher for the aggressive turn, the BVI forces are more organized and sustained during the moderate maneuver.

Constant Radius Turns

Constant radius turns at radii of 1000, 1400, and 1800 feet were flown during the ground-acoustic testing program. Both clockwise and counter clockwise turns were flown and the turns were centered on the microphone array. The airspeed was 60 KIASB. Thirteen counters were flown as shown in Table 105 for the prefix-4 data. Data segments were selected from four of these counters for the BHL data base. The time-slice relationship between the prefix-4 and BHL data bases are shown in Table 127. The counters reduced for the BHL data base are listed in Table 128.

Figure 89 shows the ground track for six of the seven BHL data base counters at radii of 1000, 1400, and 1800 feet. Microphone locations are shown as solid circles. The pilots were able to follow the specified ground track quite well, as indicated by the calculated mean and standard deviation of the turn as shown previously in Table 106. Segments selected for the

BHL data base are considerably larger than the 5-sec segments used for the BH2 data base; compare Figs. 77 and 89. In addition, for the 1400-ft radius turn, the two segments selected are essentially continuous as are the three segments chosen for the 1800-ft radius turn.

The effect of the turn rate on BVI forces on the rotor blade is examined in Fig. 90 where the filtered normal forces (17-120 harmonics) at nine radial stations are compared for the 1000- and 1800-ft constant radius turns. The comparison is based on one revolution of data. On the advancing side the BVI forces are remarkably similar and there is little difference between the two turns. On the retreating side, however, the BVI forces are strongest for the 1000-ft constant radius turn and are substantially reduced for the 1800-ft turn.

Table 110. – Microphone layouts for ground-acoustic testing.

Microphone	Standard Array		Non-standard Array	
	X-position ft	Y-position ft	X-position ft	Y-position ft
1	0.0	0.0	0.0	0.0
2	0.0	44.1	0.0	200.0
3	0.0	91.0	0.0	400.0
4	0.0	144.3	0.0	600.0
5	0.0	209.8	0.0	800.0
6	0.0	320.0	0.0	1000.0
7	0.0	561.5	0.0	1200.0
8	0.0	1417.8	0.0	1400.0
9	0.0	–44.1	0.0	–200.0
10	0.0	–91.0	0.0	–400.0
11	0.0	–144.3	0.0	–600.0
12	0.0	–209.8	0.0	–800.0
13	0.0	–320.0	0.0	–1000.0
14	0.0	–561.5	0.0	–1200.0
15	0.0	–1417.8	0.0	–1400.0
16	200.0	0.0	200.0	0.0
17	400.0	0.0	400.0	0.0
18	600.0	0.0	600.0	0.0

Table 111. – Time slices for level flight cases in prefix-4 and BHL data bases.

Prefix-4 Data Base			BHL Data Base		
COUNTER	Start Time sec	End Time sec	COUNTER	Start Time sec	End Time sec
49104	0.00	31.69	9104	6.58	24.77
49121	0.00	35.23	9121	4.72	27.91
49204	0.00	48.20	9204	0.00	47.76
49310	0.00	22.25	9310	4.90	19.09
49317	0.00	32.51	9317	0.00	27.09
49421	0.00	22.95	9421	0.00	17.09
49814	0.00	22.11	9814	0.91	19.39

Table 112. – Level flight cases from ground-acoustic testing; BHL data base.

FLIGHT	COUNTER	DESCRIPTION	DURATION
91	9104	LEVEL, 104 KIASB, RUN 140	18.19 Seconds
91	9121	LEVEL, 80 KIASB, RUN 130	23.19 Seconds
92	9204	LEVEL, 41 KIASB, RUN 110	47.86 Seconds
93	9310	LEVEL, 145 KIASB, RUN 160	14.19 Seconds
93	9317	LEVEL, 60 KIASB RUN 120	27.19 Seconds
94	9421	LEVEL, 102 KIASB, RUN 141	17.24 Seconds
98	9814[a]	LEV,100KIASB,CON.FIX,RUN143	18.48 Seconds

[a]No tracking data.

Table 113. – Flight path and tip-path-plane angles for level flight cases in ground-acoustic testing; BHL data base.

COUNTER	DESCRIPTION	γ deg	$S_e(\gamma)$ deg	α_{TPP} deg	$\sigma(\alpha_{TPP})$, deg
9104	LEVEL, 104 KIASB, RUN 140	0.37	1.14	–5.83	0.47
9121	LEVEL, 80 KIASB, RUN 130	–0.38	1.57	–3.18	0.97
9204	LEVEL, 41 KIASB, RUN 110	–0.28	12.74	–1.00	2.57
9310	LEVEL, 145 KIASB, RUN 160	0.49	0.95	–12.01	0.29
9317	LEVEL, 60 KIASB RUN 120	–0.04	3.54	–2.64	0.88
9421	LEVEL, 102 KIASB, RUN 141	–0.33	0.98	–5.71	0.76

Table 114. – Time slices for climbing flight cases in prefix-4 and BHL data bases.

	Prefix-4 Data Base			BHL Data Base	
COUNTER	Start Time sec	End Time sec	COUNTER	Start Time sec	End Time sec
49113	0.00	35.83	9113	7.47	35.93
49119	0.00	29.04	9119	5.92	29.04
49120	0.00	27.92	9120	6.89	28.01
49123	0.00	27.24	9123	3.39	27.34
49429	0.00	30.08	9429	4.90	30.17
49507	0.00	27.28	9507	5.90	27.09
49509	0.00	24.05	9509	5.91	24.10
49510	0.00	25.13	9510	1.90	25.09
49511	0.00	24.41	9511	6.90	24.09
49512	0.00	34.36	9512	4.90	34.09
49513	0.00	30.82	9513	7.90	30.09
49515	0.00	21.26	9515	0.90	20.09
49518	0.00	41.42	9518	6.91	41.10
49519	0.00	41.08	9519	9.90	41.09
49522	0.00	47.46	9522	10.90	47.09
49525	0.00	59.23	9525	17.90	57.09
49530	0.00	27.57	9530	9.90	27.09

Table 115. – Climbing flight cases from ground-acoustic testing; BHL data base.

FLIGHT	COUNTER	DESCRIPTION	DURATION
91	9113	CLIMB,9 DEG,60 KIASB,RUN 461	28.26 Seconds
91	9119[a]	CLIMB,6 DEG,80 KIASB,RUN 490	23.12 Seconds
91	9120	CLIMB,9DEG,100 KIASB,RUN 550	21.00 Seconds
91	9123	CLIMB,9 DEG,80 KIASB,RUN 510	20.93 Seconds
94	9429	ASCENT,6DEG,60KIASB, RUN 450	25.08 Seconds
95	9507	ASCENT,7DEG,80KIASB, RUN 500	23.75 Seconds
95	9509	ASCENT,6DEG,100KIASB,RUN 540	18.00 Seconds
95	9510	ASCENT,3DEG,80KIASB, RUN 480	23.00 Seconds
95	9511	ASCENT,12DEG,80KIASB,RUN 520	16.99 Seconds
95	9512	ASCENT,3DEG,60KIASB, RUN 440	29.00 Seconds
95	9513	ASCENT,12DEG,60KIASB,RUN 470	22.00 Seconds
95	9515	ASCENT,3DEG,100KIASB,RUN 530	19.00 Seconds
95	9518	ASCENT,9DEG,40KIASB, RUN 420	34.00 Seconds
95	9519	ASCENT,12DEG,40KIASB,RUN 431	31.00 Seconds
95	9522	ASCENT,6DEG,40KIASB, RUN 411	36.00 Seconds
95	9525	ASCENT,3DEG,40KIASB, RUN 400	39.00 Seconds
95	9530	ASCENT,8DEG,120KIASB,RUN 570	17.00 Seconds

[a]Record contaminated.

Table 116. – Time slices for descending flight cases in prefix-4 and BHL data bases.

Prefix-4 Data Base			BHL Data Base		
COUNTER	Start Time sec	End Time sec	COUNTER	Start Time sec	End Time sec
49108	0.00	54.38	9108	–0.01	38.36
49109	0.00	40.50	9109	–0.01	27.36
49110	0.00	34.87	9110	0.00	26.21
49111	0.00	49.99	9111	0.00	43.81
49116	0.00	29.62	9116	–0.01	22.73
49118	0.00	34.98	9118	–0.01	26.87
49122	0.00	32.26	9122	–0.01	24.30
49125	0.00	36.77	9125	4.92	30.92
49320	0.00	27.98	9320	–0.14	19.99
49422	0.00	27.58	9422	–1.00	16.99
49423	0.00	32.43	9423	–0.36	20.00
49425	0.00	25.13	9425	–0.32	19.00
49427	0.00	49.01	9427	–0.37	39.00
49428	0.00	46.48	9428	–0.52	37.00
49616	0.00	24.69	9616	–0.50	24.00

Table 117. – Descending flight cases from ground-acoustic testing; BHL data base.

FLIGHT	COUNTER	DESCRIPTION	DURATION
91	9108	DESCENT,9DEG,60KIASB,RUN 260	38.37 Seconds
91	9109	DESCENT,6DEG,80KIASB,RUN 290	27.37 Seconds
91	9110	DESCENT,9DEG,100KIAB,RUN 350	26.22 Seconds
91	9111	DESCENT,12DEG,38KIAB,RUN 230	43.82 Seconds
91	9116	DESCENT,7DEG,80KIASB,RUN 300	22.74 Seconds
91	9118	DESCENT,9DEG,80KIASB,RUN 310	26.88 Seconds
91	9122	DESCENT,8DEG,120KIASB,RUN370	24.31 Seconds
91	9125	DESCENT,12DEG,80KIASB,RUN320	26.00 Seconds
93	9320	DESCENT,6DEG,100KIASB,RUN340	20.14 Seconds
94	9422	DESCENT,3DEG,60KIASB,RUN 240	18.00 Seconds
94	9423	DESCENT,3DEG,80KIASB,RUN 280	20.36 Seconds
94	9425	DESCENT,12DEG,100KIASB,RN361	19.31 Seconds
94	9427	DESCENT,6DEG,40KIASB,RUN 210	39.38 Seconds
94	9428	DESCENT,9DEG,40KIASB,RUN 220	37.52 Seconds
96	9616	DESCENT,6DEG,60KIASB,RUN 250	24.50 Seconds

Table 118. – Flight path and tip-path-plane angles for climbing flight cases in ground-acoustic testing; BHL data base.

COUNTER	DESCRIPTION	γ deg	$S_e(\gamma)$ deg	α_{TPP} deg	$\sigma(\alpha_{TPP})$, deg
9113	CLIMB,9 DEG,60 KIASB,RUN 461	7.96	6.28	–9.93	2.45
9119[a]	CLIMB,6 DEG,80 KIASB,RUN 490				
9120	CLIMB,9DEG,100 KIASB,RUN 550	8.96	11.24	–12.46	3.29
9123	CLIMB,9 DEG,80 KIASB,RUN 510	6.97	5.88	–10.97	2.08
9429	ASCENT,6DEG,60KIASB, RUN 450	6.33	7.95	–10.38	2.29
9507	ASCENT,7DEG,80KIASB, RUN 500	6.28	7.91	–9.97	2.48
9509	ASCENT,6DEG,100KIASB,RUN 540	5.53	6.57	–10.98	1.70
9510	ASCENT,3DEG,80KIASB, RUN 480	2.82	5.19	–5.74	1.49
9511	ASCENT,12DEG,80KIASB,RUN 520	11.97	6.00	–14.60	3.96
9512	ASCENT,3DEG,60KIASB, RUN 440	2.64	8.40	–5.67	2.11
9513	ASCENT,12DEG,60KIASB,RUN 470	9.48	21.52	–10.01	4.69
9515	ASCENT,3DEG,100KIASB,RUN 530	2.84	3.98	–8.81	1.03
9518	ASCENT,9DEG,40KIASB, RUN 420	8.96	6.28	–11.04	1.83
9519	ASCENT,12DEG,40KIASB,RUN 431	11.48	7.73	–12.94	2.86
9522	ASCENT,6DEG,40KIASB, RUN 411	5.95	3.81	–8.63	2.90
9525	ASCENT,3DEG,40KIASB, RUN 400	2.40	10.12	–5.58	2.56
9530	ASCENT,8DEG,120KIASB,RUN 570	8.55	3.22	–13.96	1.81

[a]Record contaminated.

Table 119. – Flight path and tip-path-plane angles for descending flight cases in ground-acoustic testing; BHL data base.

COUNTER	DESCRIPTION	γ deg	$S_e(\gamma)$ deg	α_{TPP} deg	$\sigma(\alpha_{TPP})$, deg
9108	DESCENT,9DEG,60KIASB,RUN 260	–8.50	4.10	7.23	1.23
9109	DESCENT,6DEG,80KIASB,RUN 290	–5.79	3.31	2.85	1.38
9110	DESCENT,9DEG,100KIAB,RUN 350	–9.04	1.66	4.04	1.03
9111	DESCENT,12DEG,38KIAB,RUN 230	–11.84	6.28	10.30	2.67
9116	DESCENT,7DEG,80KIASB,RUN 300	–6.36	2.67	2.90	0.68
9118	DESCENT,9DEG,80KIASB,RUN 310	–8.57	2.61	5.43	0.48
9122	DESCENT,8DEG,120KIASB,RUN370	–7.30	2.92	–0.85	0.86
9125	DESCENT,12DEG,80KIASB,RUN320	–11.77	6.82	8.50	2.18
9320	DESCENT,6DEG,100KIASB,RUN340	–6.13	1.36	1.24	0.67
9422	DESCENT,3DEG,60KIASB,RUN 240	–2.32	4.66	0.97	2.03
9423	DESCENT,3DEG,80KIASB,RUN 280	–2.51	2.36	–0.49	1.33
9425	DESCENT,12DEG,100KIASB,RN361	–11.41	4.30	6.98	3.33
9427	DESCENT,6DEG,40KIASB,RUN 210	–5.82	6.19	4.09	2.86
9428	DESCENT,9DEG,40KIASB,RUN 220	–8.44	11.65	6.92	2.97
9616	DESCENT,6DEG,60KIASB,RUN 250	–6.30	1.36	4.12	1.21

Table 120. – Sweep in tip-path-plane angle at $\mu = 0.20$ for ground-acoustic testing; BHL data base.

COUNTER	DESCRIPTION	α_{TPP} deg	Local α_{TPP} deg	Start Time, sec
9511	ASCENT,12DEG,80KIASB,RUN 520	–14.60	–16.94	6.43
9123	CLIMB,9 DEG,80 KIASB,RUN 510	–10.97	–10.46	19.15
9510	ASCENT,3DEG,80KIASB, RUN 480	–5.74	–6.33	20.11
9121	LEVEL, 80 KIASB, RUN 130	–3.18	–3.88	18.55
9423	DESCENT,3DEG,80KIASB,RUN 280	–0.49	–1.29	13.68
9116	DESCENT,7DEG,80KIASB,RUN 300	2.90	3.60	2.87
9118	DESCENT,9DEG,80KIASB,RUN 310	5.43	5.19	4.18
9125	DESCENT,12DEG,80KIASB,RUN320	8.50	10.20	2.76

Table 121. – Time slices for hover cases in prefix-4 and BHL data bases.

Prefix-4 Data Base			BHL Data Base		
COUNTER	Start Time sec	End Time sec	COUNTER	Start Time sec	End Time sec
49404	0.00	25.02	9404	5.00	10.00
49405	0.00	24.71	9405	5.00	10.00
49406	0.00	24.94	9406	5.00	10.00
49407	0.00	24.59	9407	5.01	10.00
49408	0.00	25.34	9408	5.01	9.99
49409	0.00	14.99	9409	5.01	10.00
49410	0.00	24.50	9410	5.01	9.99
49411	0.00	24.87	9411	5.00	9.99
49412	0.00	25.13	9412	5.01	10.00
49413	0.00	24.66	9413	4.96	9.99
49414	0.00	24.67	9414	5.01	10.00
49415	0.00	24.47	9415	5.01	10.00
49416	0.00	24.38	9416	5.01	10.00

Table 122. – Hover cases from ground-acoustic testing; BHL data base.

FLIGHT	COUNTER	DESCRIPTION	DURATION
94	9404	HOVER, HDG=173, RUN 602	5.00 Seconds
94	9405	HOVER, HDG=188, RUN 607	5.00 Seconds
94	9406	HOVER, HDG=203, RUN 610	4.99 Seconds
94	9407[a]	HOVER, HDG=218, RUN 615	4.99 Seconds
94	9408[a]	HOVER, HDG=233, RUN 620	4.99 Seconds
94	9409	HOVER, HDG=248, RUN 625	4.99 Seconds
94	9410	HOVER, HDG=263, RUN 630	4.99 Seconds
94	9411	HOVER, HDG=278, RUN 635	4.99 Seconds
94	9412	HOVER, HDG=293, RUN 640	4.99 Seconds
94	9413	HOVER, HDG=308, RUN 645	5.03 Seconds
94	9414	HOVER, HDG=323, RUN 650	4.99 Seconds
94	9415	HOVER, HDG=338, RUN 655	4.99 Seconds
94	9416	HOVER, HDG=353, RUN 660	4.99 Seconds

[a]Radar tracking data erroneous.

Table 123. – Time slices for moderate heading turns in prefix-4 and BHL data bases.

Prefix-4 Data Base			BHL Data Base		
COUNTER	Start Time sec	End Time sec	COUNTER	Start Time sec	End Time sec
49206	0.00	26.55	9206	3.63	18.63
49207	0.00	28.13	9207	2.30	23.30
49210	0.00	33.88	9210	2.20	32.20
49211	0.00	23.51	9211	0.13	16.13
49213	0.00	20.75	9213	–0.01	17.74
49214	0.00	27.87	9214	0.31	23.31
49215	0.00	29.62	9215	0.65	26.64
49708	0.00	24.22	9708	0.00	18.00
49709	0.00	26.86	9709	3.01	23.00
49712	0.00	27.76	9712	0.00	21.00
49713	0.00	30.66	9713	0.00	23.00
49724	0.00	22.94	9724	–0.03	21.00
49908	0.00	35.42	9908	5.69	25.00

Table 124. – Moderate heading turns from ground-acoustic testing; BHL data base.

FLIGHT	COUNTER	DESCRIPTION	DURATION
92	9206	TURN,25 DEG,60 KIASB,RUN 701	15.00 Seconds
92	9207	TURN,45 DEG,60 KIASB,RUN 720	21.00 Seconds
92	9210	TURN,90 DEG,60 KIASB,RUN 740	30.00 Seconds
92	9211	TURN,15 DEG,80 KIASB,RUN 702	15.99 Seconds
92	9213	TURN,45 DEG,80 KIASB,RUN 721	17.75 Seconds
92	9214	TURN,60 DEG,80 KIASB,RUN 731	23.00 Seconds
92	9215	TURN,90 DEG,80 KIASB,RUN 741	26.00 Seconds
97	9708	TURN,RT 30DG,60KIASB,RUN 746	18.00 Seconds
97	9709	TURN,RT 45DG,60KIASB,RUN 750	20.00 Seconds
97	9712	TURN,LT 45DG,60KIASB,RUN 710	21.00 Seconds
97	9713	TURN,LT 60DG,60KIASB,RUN 720	23.00 Seconds
97	9724	TURN LT 60DG,60KIASB,RUN 725	21.04 Seconds
99	9908	RT TURN 60DEG,60KIASB,RUN761	19.31 Seconds

Table 125. – Time slices for aggressive heading turns in prefix-4 and BHL data bases.

Prefix-4 Data Base			BHL Data Base		
COUNTER	Start Time sec	End Time sec	COUNTER	Start Time sec	End Time sec
49716	0.00	27.55	9716	3.01	26.00
49719	0.00	29.63	9719	1.00	18.99
49842	0.00	26.84	9842	4.00	23.00
49909	0.00	22.16	9909	5.00	20.00
49914	0.00	25.51	9914	9.15	22.00
49920	0.00	25.20	9920	4.01	22.00
49924	0.00	27.39	9924	10.50	24.99

Table 126. – Aggressive heading turns from ground-acoustic testing; BHL data base.

FLIGHT	COUNTER	DESCRIPTION	DURATION
97	9716	CA TURN L60DG,60KIASB,RUN800	23.00 Seconds
97	9719	CA TURN R45DG,60KIASB,RUN830	18.00 Seconds
98	9842	CA LT TURN 30DEG RUN 700	19.00 Seconds
99	9909	CA TURN,L30DG,60KIASB,RUN780	15.00 Seconds
99	9914	CA TURN,R60DG,60KIASB,RUN840	12.84 Seconds
99	9920	CA TURN,L90DG,60KIASB,RUN810	18.00 Seconds
99	9924	CA TURN,R90DG,60KIASB,RUN771	14.49 Seconds

Table 127. – Time slices for constant radius turns in prefix-4 and BHL data bases.

Prefix-4 Data Base			BHL Data Base		
COUNTER	Start Time sec	End Time sec	COUNTER	Start Time sec	End Time sec
49618	0.00	117.64	9620	50.01	62.40
49618	0.00	117.64	9621	62.30	90.40
49618	0.00	117.64	9622	90.30	108.00
49632	0.00	77.87	9633	21.12	44.01
49632	0.00	77.87	9634	43.92	67.11
49836	0.00	50.90	9836	0.01	30.00
49839	0.00	56.38	9840	26.00	56.00

Table 128. – Constant radius turns from ground-acoustic testing; BHL data base.

FLIGHT	COUNTER	DESCRIPTION	DURATION
96	9620	CW TURN,1800',58KIASB,RUN880	12.40 Seconds
96	9621	CW TURN,1800',58KIASB,RUN880	28.10 Seconds
96	9622	CW TURN,1800',58KIASB,RUN880	17.70 Seconds
96	9633	CCW TURN,1400',60KIASB,RN900	22.90 Seconds
96	9634	CCW TURN,1400',60KIASB,RN900	23.20 Seconds
98	9836	TURN CW 1000'RAD. R860 SEG1	30.00 Seconds
98	9840	TURN CCW 1000'RAD.R890 SEG 2	30.00 Seconds

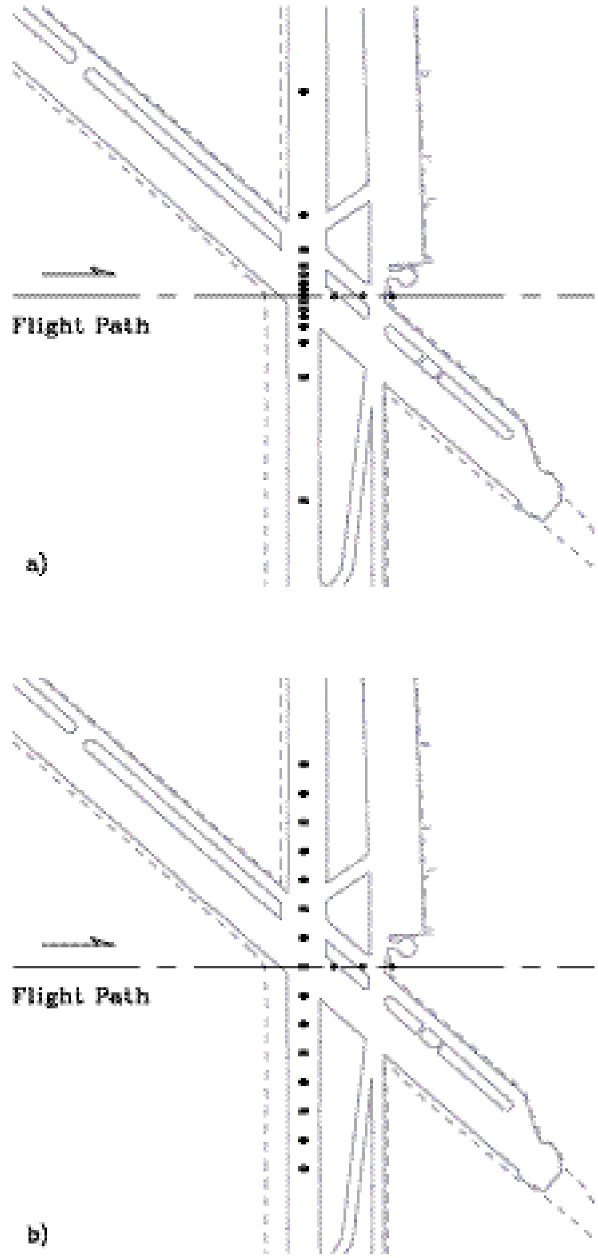

Figure 79. – Microphone layouts at Crows Landing NAAF. a) standard array; b) non-standard array.

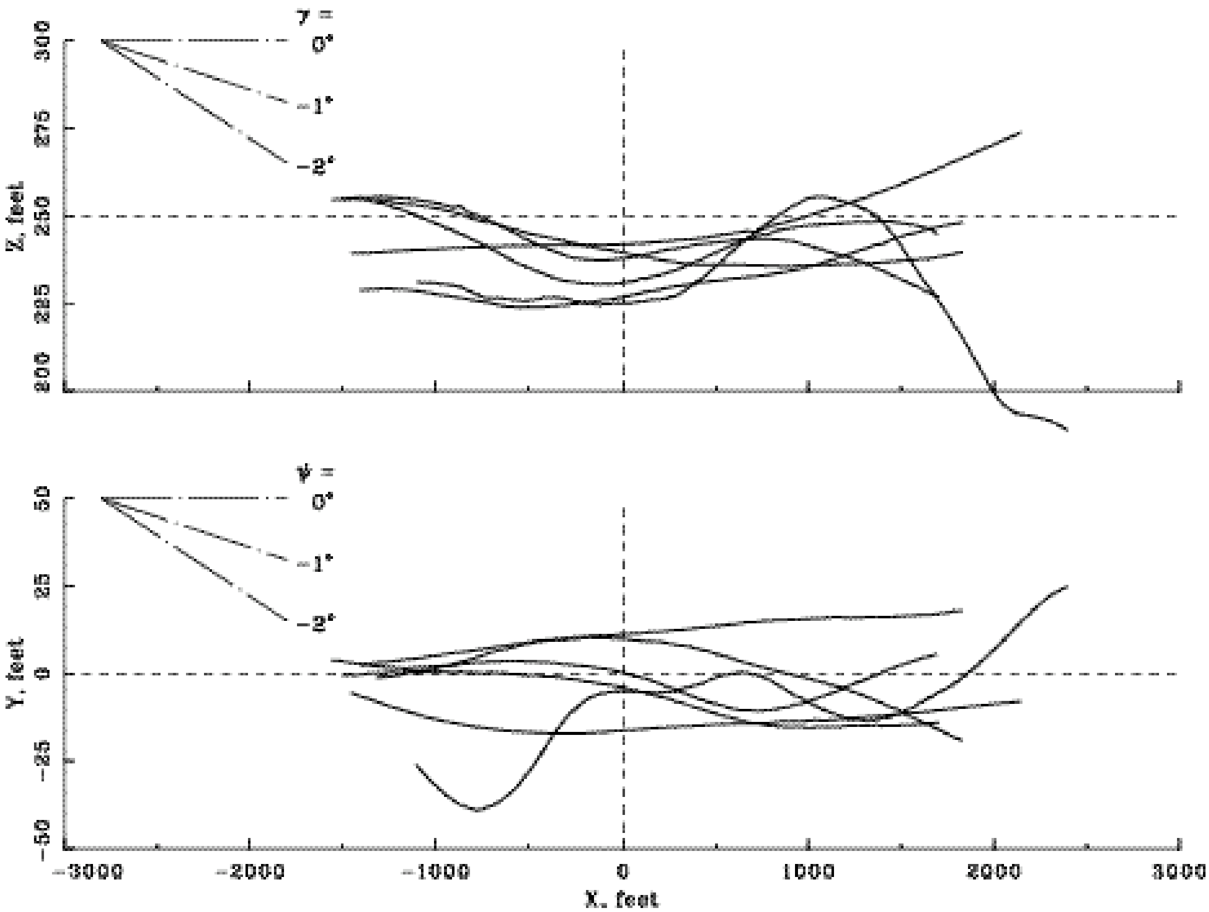

Figure 80. – Z- and Y-position data as a function of X-position for level flight data in ground-acoustic tests; BHL data base. The zero reference is the center of the acoustical array. Vertical and lateral scales have a 20X exaggeration.

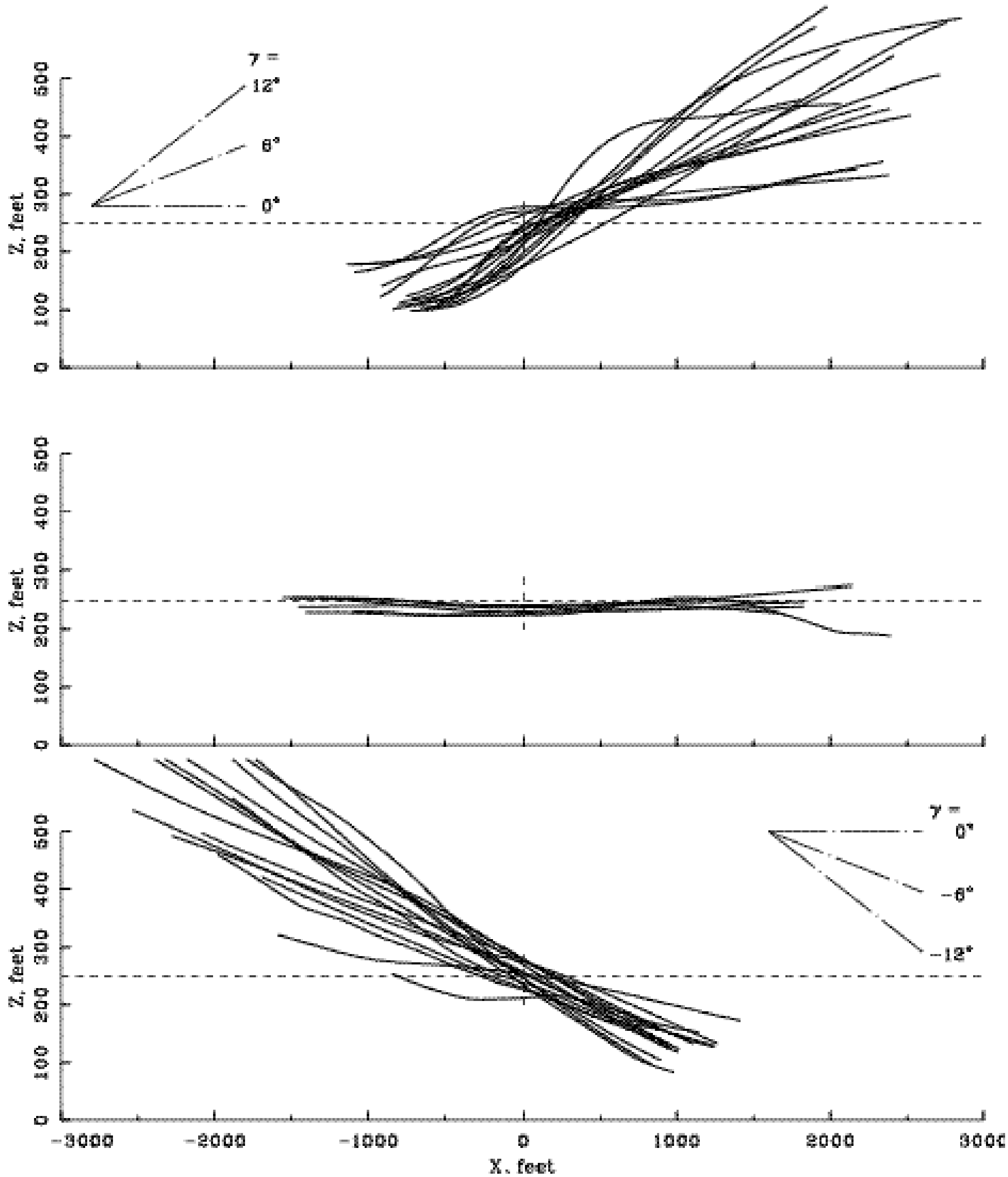

Figure 81. – Vertical position as a function of horizontal position during climb, level flight and descending flight conditions as obtained with a laser tracker. Vertical scale has a 3.75X exaggeration.

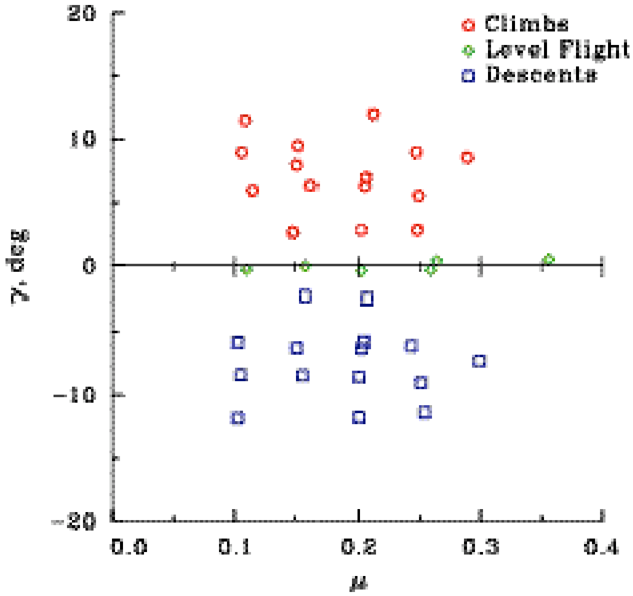

Figure 82. – Measured flight path angles for climbs, level flight, and descending flight conditions during ground-acoustic testing; BHL data base.

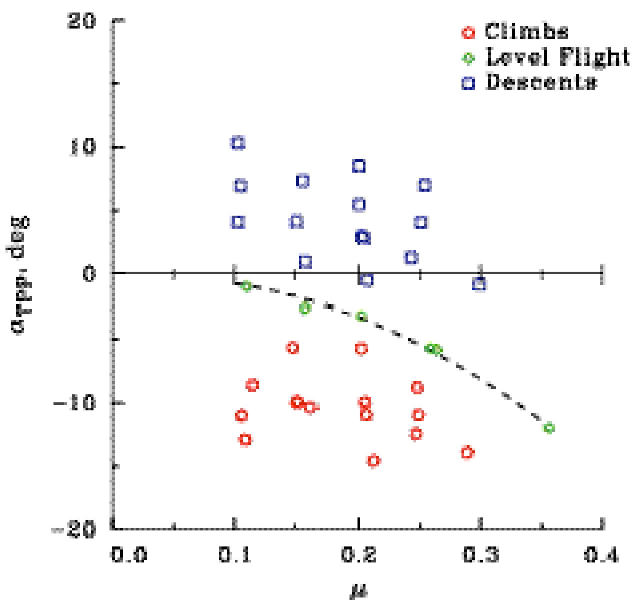

Figure 83. – Measured tip-path-plane angles for climbs, level flight, and descending flight conditions during ground-acoustic testing; BHL data base. Fitted line shows level flight conditions.

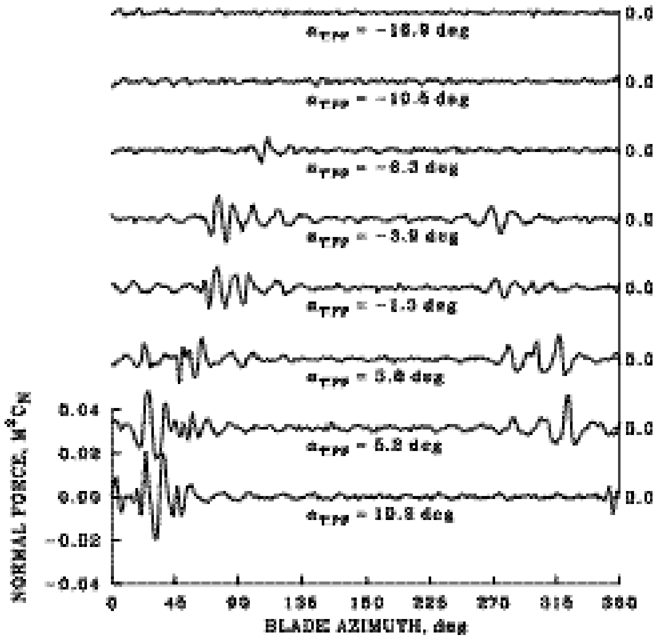

Figure 84. – Filtered time histories of normal force at 0.865*R* at an advance ratio of 0.2 shown as a function of tip-path-plane angle; 17–120 harmonics.

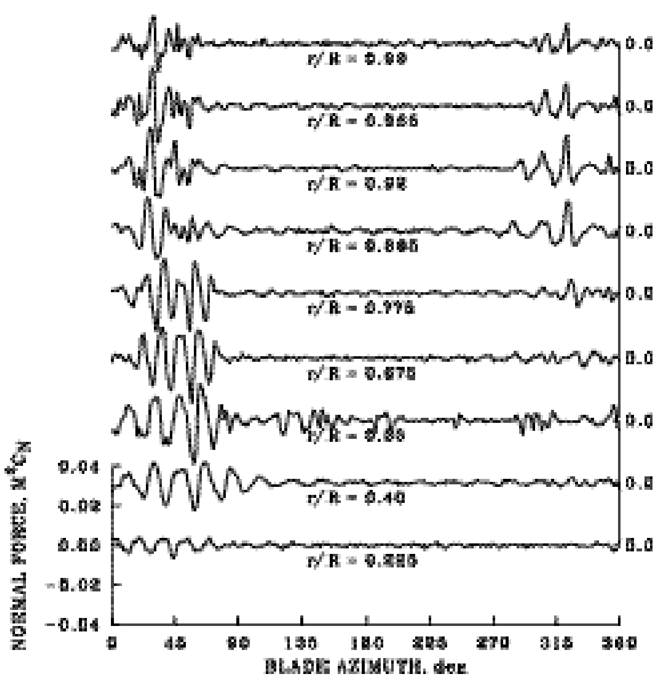

Figure 85. – Filtered time histories of normal force as a function of blade radial station at at α_{TPP} = 5.2 deg, μ = 0.2; 17–120 harmonics.

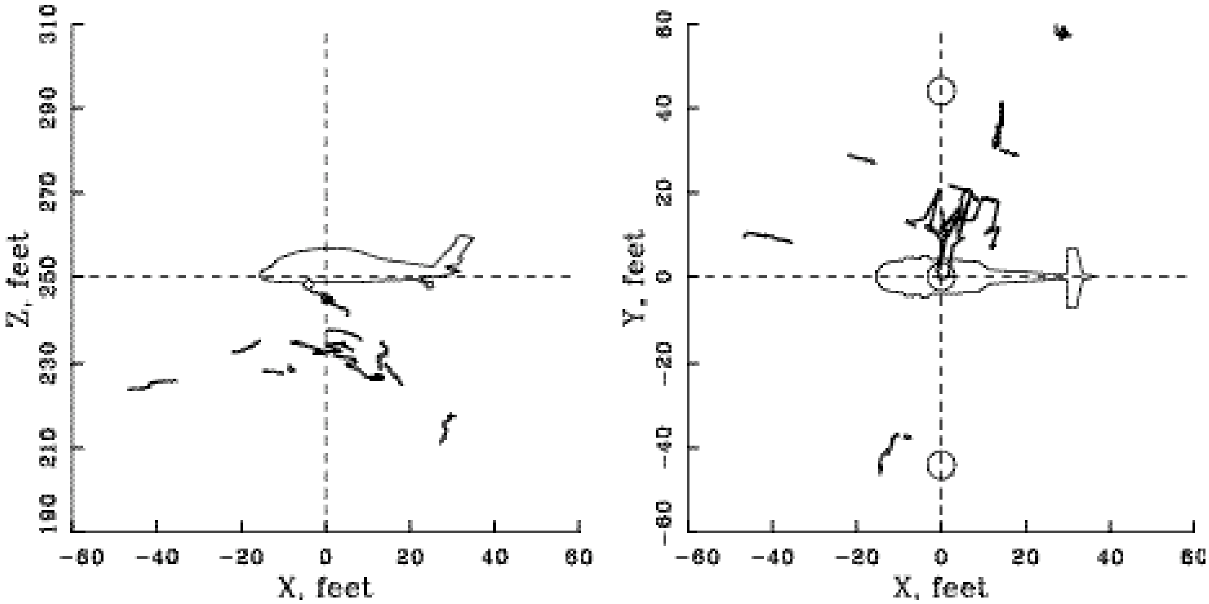

Figure 86. – Tracking data for ground-acoustic hover points for BHL data base. Outline of UH–60A is shown only for scale; the heading was changed between each test point.

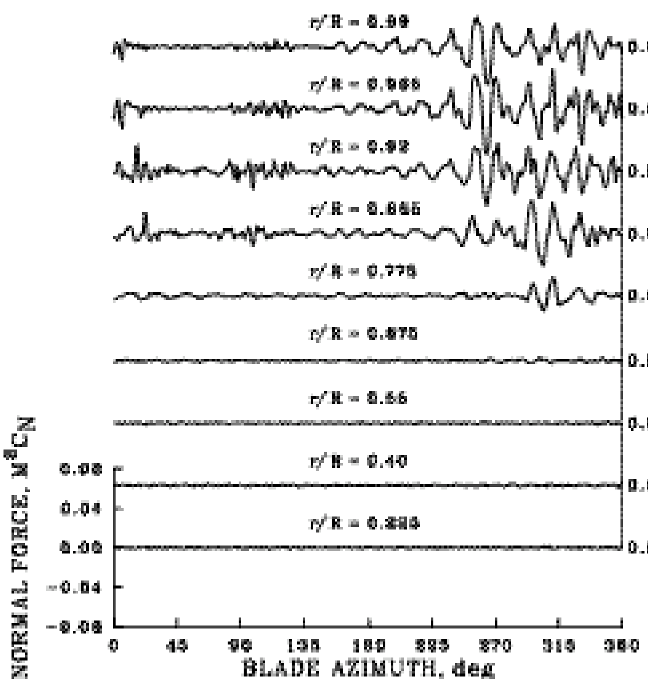

Figure 87. –. Filtered time histories of normal force as a function of blade radial station for hover in wind; 17–120 harmonics (Counter 9406).

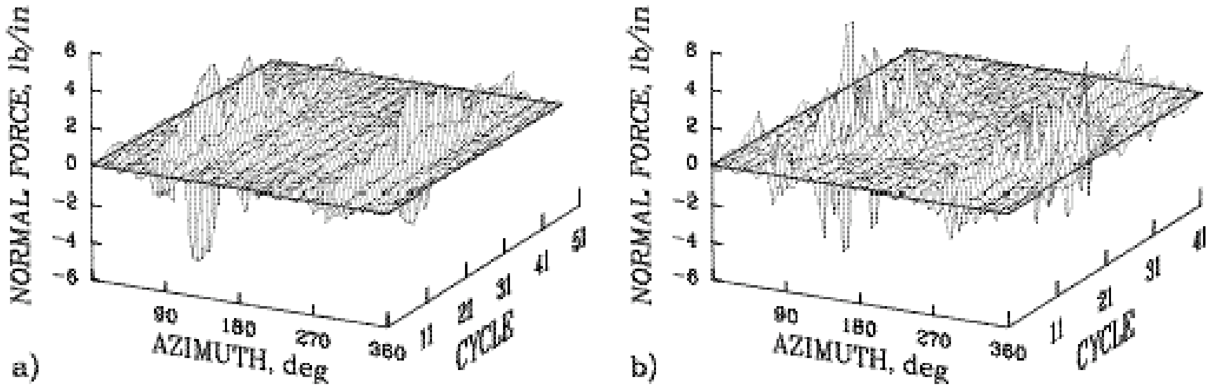

Figure 88. – Filtered time histories of normal force at 0.92R during moderate and aggressive 60 deg right turns with an approach speed of 60 KIASB. a) moderate turn, Counter 9908; b) aggressive turn, Counter 9914.

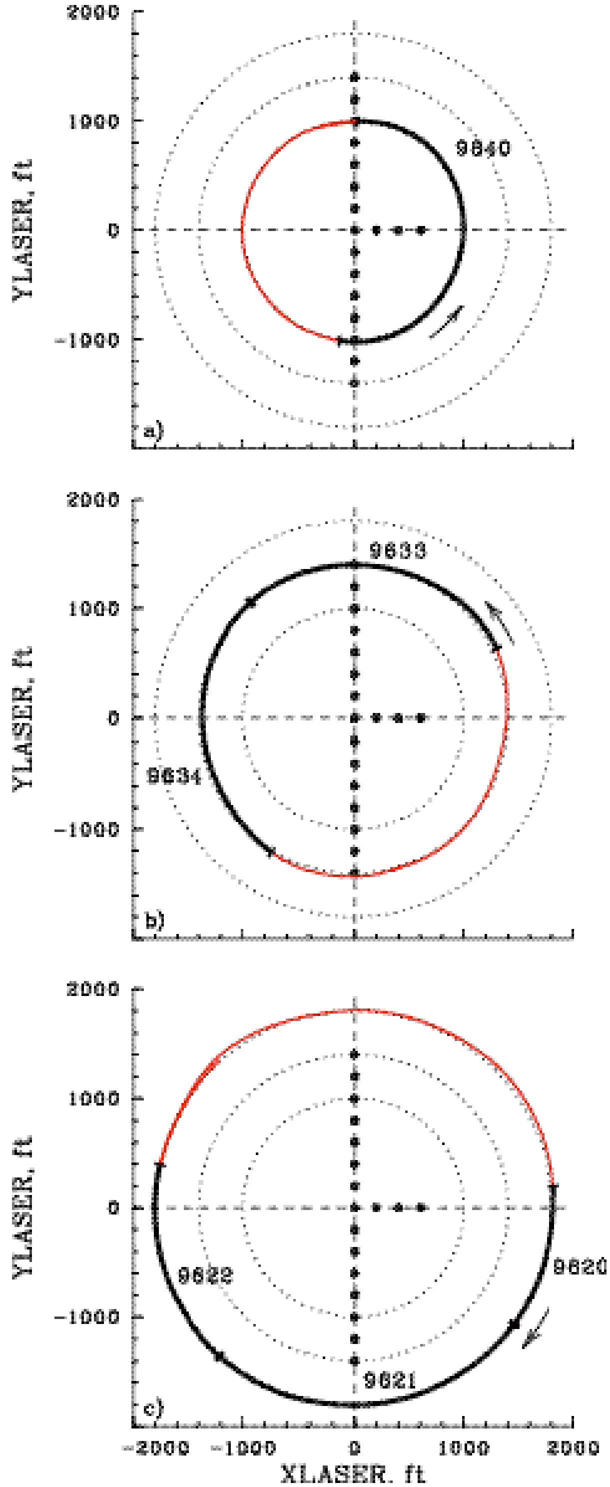

Figure 89. – X- and y-position track for constant radius turns on three radii, including selected BHL data base segments. Segment boundaries indicated by crossbars. Solid circles show microphone array locations for Flights 96 to 99. a) 1000-ft radius (Counter 49839); b) 1400-ft radius (Counter 49632); c) 1800-ft radius (Counter 49618).

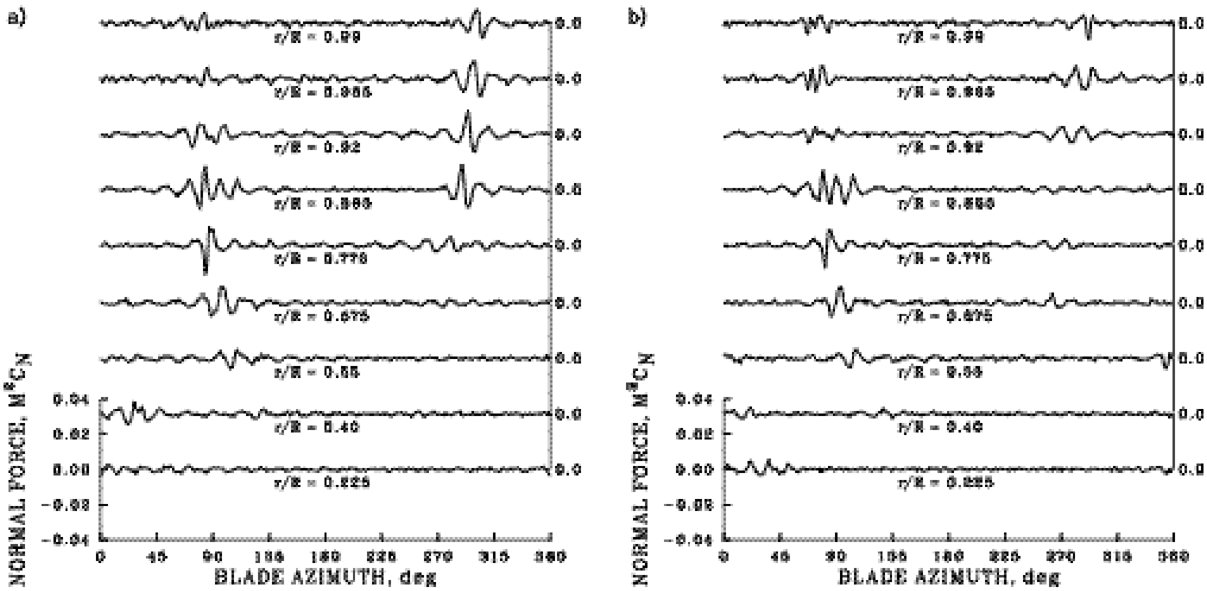

Figure 90. – Filtered time histories of normal force as a function of blade radial station for constant radius turns; 17–120 harmonics. a) 1000-foot radius (Counter 9840); b) 1800-foot radius (Counter 9621).